



ELSEVIER

Physica A 316 (2002) 19–28

PHYSICA A

www.elsevier.com/locate/physa

# Fluctuation-induced mound coarsening in two dimensions

Jacques G. Amar<sup>a,\*</sup>, Daniel J. Baxter<sup>b,1</sup>

<sup>a</sup>Department of Physics and Astronomy, University of Toledo, Toledo, OH 43606, USA

<sup>b</sup>Department of Physics, Carleton College, Northfield, MN 55057, USA

Received 02 May 2002

---

## Abstract

The effects of deposition noise on two-dimensional mound coarsening with slope selection are studied using both continuum and discrete models. Our continuum model may also be considered as a model of two-dimensional polycrystalline growth with a preferred facet orientation. In agreement with recent scaling arguments, we find  $n = \beta = \frac{1}{3}$ , where  $n$  is the mound coarsening exponent and  $\beta$  is the surface roughening exponent. We also find  $\delta = \frac{1}{3}$  where  $\delta$  is the facet length coarsening exponent. These results are compared with simulation results obtained using a discrete model in which deposition noise and diffusion have been included, but island nucleation and mass transfer between mounds are assumed to be negligible. In the presence of an interfacial diffusion barrier, the surface exhibits a self-affine morphology and Edwards–Wilkinson scaling behavior ( $\beta = \frac{1}{4}$ ) while the average facet length is constant ( $\delta = 0$ ). However, in the absence of a barrier to interfacial diffusion, we again find a mound-like morphology and coarsening with  $n = \beta = \frac{1}{3}$ , while the average facet length increases logarithmically with film thickness. The slow growth of the facet length in this case may also explain the absence of island nucleation in polycrystalline growth. Our results may also be useful in the development of improved continuum and discrete models of polycrystalline growth.

© 2002 Elsevier Science B.V. All rights reserved.

PACS: 81.15.Aa; 68.55.–a; 68.43.Jk; 81.10.–h

Keywords: Epitaxial growth; Mound coarsening; Polycrystalline growth; Phase separation

---

---

\* Corresponding author. Tel.: +1-419-530-2259; fax: +1-419-530-2723.

E-mail address: [jamar@physics.utoledo.edu](mailto:jamar@physics.utoledo.edu) (J.G. Amar).

<sup>1</sup> Current address: School of Engineering and Applied Science, Washington University, St. Louis, MO, USA.

## 1. Introduction

The growth and coarsening of mounds during homoepitaxial growth on singular surfaces has attracted considerable interest over the past several years [1,2]. In particular, mound formation has been observed in homoepitaxial growth of materials ranging from semiconductors [3–5] to metals and metal alloys [6–13]. One reason for the interest has been the desire to control instabilities during the growth process in order to produce either atomically flat or nanostructured surfaces.

While the origin of the mound instability is understood to be the existence of diffusion bias [14] (due, for example, to an Ehrlich–Schwoebel barrier to diffusion over steps [15]) the asymptotic mound coarsening and surface roughening behavior are less well understood. For example, simulations of mound coarsening with a selected slope indicate that in three dimensions the coarsening behavior can depend on the strength of the Ehrlich–Schwoebel barrier [16,17], surface symmetry [18,19], as well as on the presence or absence of relaxation mechanisms such as corner diffusion [17].

Recently, Tang and co-workers [20,21] have presented scaling arguments for the coarsening behavior corresponding to two particular mechanisms of mound coalescence—bonding energy driven coalescence, and coalescence due to deposition noise. For the case of bonding energy dominated coarsening in three dimensions the value  $\beta = n = \frac{1}{4}$  was obtained while for the case of noise-driven coarsening in the presence of slope selection, the result  $\beta = n = 1/(d + 1)$  (where  $d$  is the dimensionality of the system) was obtained. The latter result implies  $\beta = n = \frac{1}{3}$  in two dimensions, in agreement with continuum theories of isotropic mound coarsening [22,23] which take into account both ‘equilibrium’ effects (such as surface curvature and detachment [24]) and kinetic effects such as diffusion bias. However, no direct tests of the effects of deposition noise alone on the mound coarsening behavior have been carried out.

Here, we present the results of simulations of both continuum and discrete models of two-dimensional mound growth with angle selection in which the coarsening is entirely due to deposition noise while other effects such as mass transfer due to detachment and island nucleation are assumed to be negligible. Our continuum and discrete models may also be considered to be models of two-dimensional polycrystalline growth with a single set of symmetric preferred facet orientations. In agreement with the scaling arguments of Ref. [20] for noise-assisted coarsening in two dimensions, we find  $n = \beta = \frac{1}{3}$  for the continuum model. In order to better understand the connection between the coarsening behavior and the microscopic dynamics, we have also carried out simulations of a discrete model of mound coarsening in which again deposition noise plays a primary role, and the effects of nucleation and surface relaxation due to detachment are not included. In this case, we find two different universality classes. In the presence of an interfacet diffusion barrier, the surface exhibits a self-affine morphology and Edwards–Wilkinson [25] scaling behavior ( $\beta = \frac{1}{4}$ ) while the average facet length is constant and no coarsening is observed. However, in the absence of a barrier to interfacet diffusion, we again find a mound-like morphology and coarsening with  $n = \beta = \frac{1}{3}$ . In this case, the average facet length is found to increase logarithmically with the film thickness. Possible extensions of our models to the study of polycrystalline growth with random orientations or shadowing are also discussed.

## 2. Continuum model

In order to simulate the effects of deposition noise within a continuum model we have developed the following ‘ghost-particle’ model. The surface is represented by a set of lines with a fixed mound or facet angle as shown in Fig. 1. At each stage of the deposition process a random position along the substrate (see arrow in Fig. 1) is selected for deposition of the next particle. This determines the facet upon which deposition is to take place. The corresponding facet is then propagated in such a manner as to ensure a fixed growth ‘area’ at each growth step corresponding to the area of each particle as shown in Fig. 1. In particular, at each deposition step, the film gains an area of one (in units of the particle area). Fig. 1(a) shows the results of a typical particle deposition, while Fig. 1(b) shows a deposition in which a facet is overrun by its neighbor.

As an initial surface configuration, we assumed a sequence of equal-sized ‘mounds’ or triangles with facet length equal to one unit while the facet angle was assumed to be  $45^\circ$ . If we think of the deposited ‘ghost’ particle as a square of side one rotated by  $45^\circ$ , this makes the very early stages of growth similar to the single-step model [26]. In order to study the resulting coarsening behavior, two measures of the average

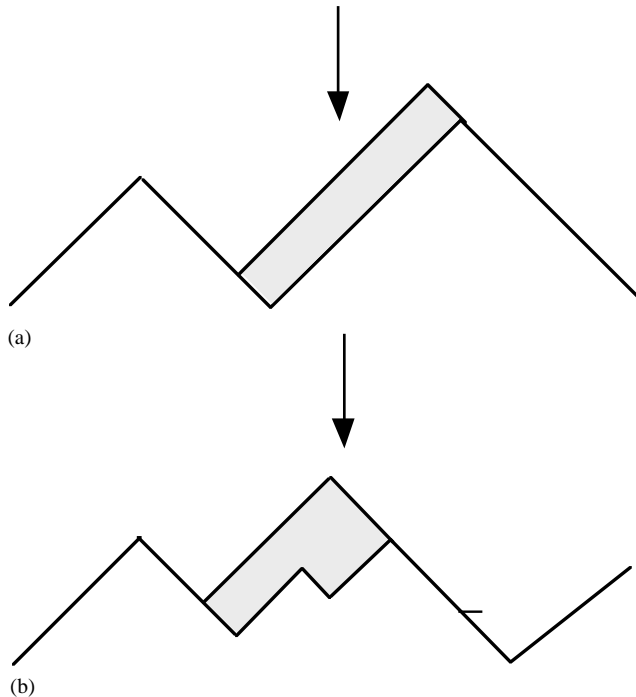


Fig. 1. Diagram showing motion of facets after a single deposition event in ghost-particle model. Arrow corresponds to position of deposited particle while shaded area shows growth of facet after a deposition step: (a) a single facet is propagated, and (b) facet is overrun by its neighbor.



Fig. 2. Sequence of configurations in ghost-particle model (bottom to top) corresponding to (a) starting configuration, (b) 1.25 layers, and (c) 3.75 layers.

mound size were used—the r.m.s. surface width  $w = \langle (h - \langle h \rangle)^2 \rangle^{1/2}$ , and the average facet length  $f$ . The surface width was used to obtain a ‘roughening’ exponent  $\beta$  where  $w \sim \langle h \rangle^\beta$ , while the facet length  $f$  was used to obtain a coarsening exponent  $n$ , where  $f \sim \langle h \rangle^n$ . Since a fixed facet angle is assumed, one expects that  $\beta = n$ . In our simulations, periodic boundary conditions were used.

Fig. 2 shows a typical sequence of configurations for a small system size with increasing film thickness. In the absence of deposition noise, one expects that the initial surface configuration will propagate essentially unchanged. However, as can be seen, due to the presence of deposition noise there is significant mound coarsening. Also, as shown by the top picture in Fig. 2, despite the ‘small area’ cutoff corresponding to the size of a particle, the facet length can be arbitrarily small.

In order to accurately measure the coarsening behavior, simulation of a large system with an initial state of 2000 triangles was carried out. In this simulation, 21,000 ghost particles were deposited corresponding to an average film thickness of 10.5 layers. Fig. 3 shows the corresponding results for the growth of the average facet size and surface width as a function of film thickness. As can be seen, in agreement with the scaling arguments we find  $\beta \simeq n \simeq \frac{1}{3}$ .

### 3. Discrete model

In order to better understand the results obtained in our continuum model we have also studied a discrete model of mound coarsening in which both island nucleation and mass transfer between mounds due to detachment are excluded but deposition noise is included. One motivation for developing such a discrete model is the fact that in three dimensions such a model is likely to be much easier to simulate than a continuum model. In particular, we have considered a variation of the single-step model [26] in which diffusion along a facet to the nearest ‘kink’ site is allowed.

As in our continuum model, the starting configuration corresponds to a sequence of alternate heights (0,1), which may be represented by a sequence of rotated squares on a lattice (see Fig. 4(a)). At each deposition step, a deposition column is randomly

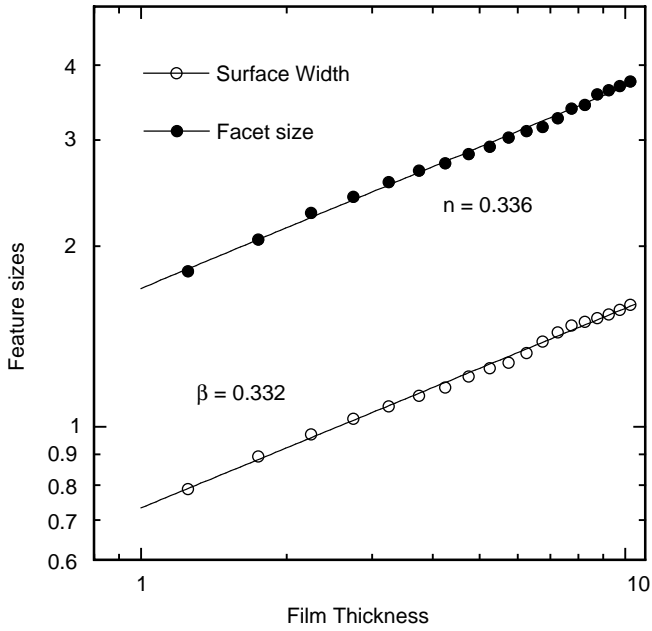


Fig. 3. Feature size as a function of film thickness obtained from continuum ghost-particle model.

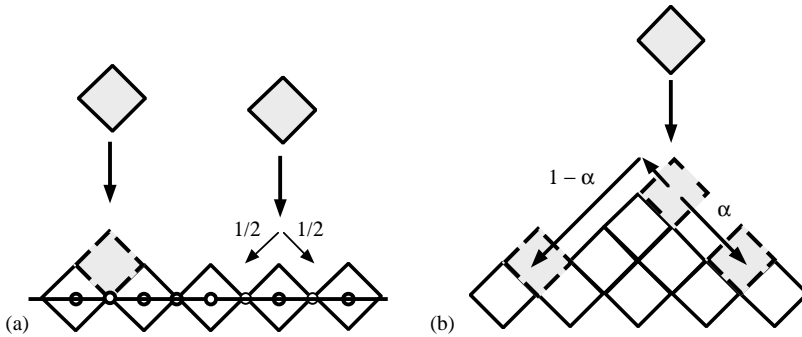


Fig. 4. Diagram showing (a) initial configuration and deposition sites (circles) and (b) diffusion in single-step model.

selected and a particle is deposited in that column. While in the original single-step model [26], deposition in columns which are not local minima was rejected since they do not satisfy the single-step restriction  $|h_{i+1} - h_i| \leq 1$ , in our model particles not deposited at kink sites are allowed to diffuse to a nearby local minimum or kink site.

In particular, we considered two versions of this single-step model. In the first version, particles may only diffuse downhill to the nearest local minimum, i.e., there is an infinite barrier to interfacet diffusion. In this version, if a particle is deposited at a site corresponding to a local maximum (e.g. the column to the left of the particle being

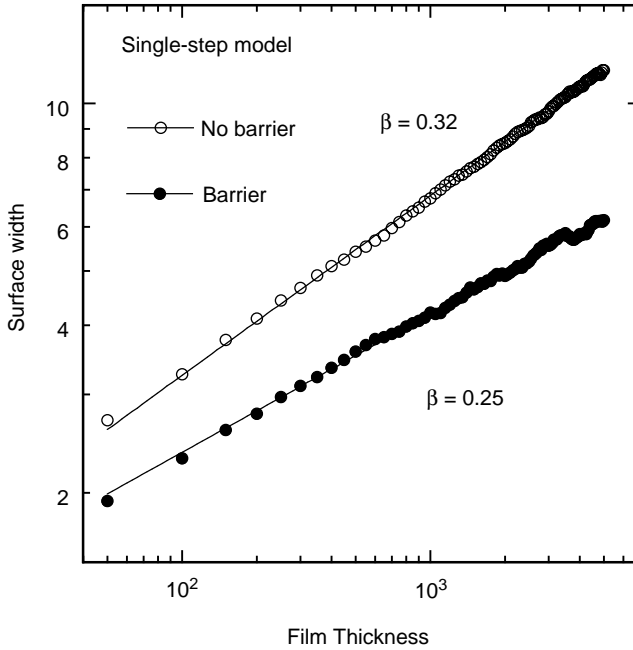


Fig. 5. Single-step model with barrier.

deposited in Fig. 4(b)), then it is assumed to diffuse with equal probability to the local minimum on the right or on the left. In the second version, particles may diffuse to local minima on either side of the nearest local maximum, i.e., there is no barrier to interfacet diffusion. Rather than actually carry out the diffusion, we have calculated the probability  $\alpha = n_R/(n_L + n_R)$  ( $1 - \alpha = n_L/(n_L + n_R)$ ) of going to the kink site to the right (left) as a function of the number of hops  $n_R$  ( $n_L$ ) to the nearest kink sites on the right (left), respectively [27,28]. For the example shown in Fig. 4(b),  $\alpha = 1$  in the presence of an interfacet diffusion barrier while  $\alpha = \frac{1}{3}$  in the absence of an interfacet diffusion barrier.

In order to characterize the surface morphology, the height–height correlation function  $G(x) = \langle \tilde{h}(0)\tilde{h}(x) \rangle$  (where  $\tilde{h}(x) = h(x) - \langle h \rangle$ ) and the r.m.s. surface width  $w = [G(0)]^{1/2}$  were calculated as a function of film thickness. The lateral feature size  $r_c$  was also calculated by determining the zero-crossing of  $G(x)$  in order to determine the lateral coarsening exponent ( $r_c \sim \langle h \rangle^n$ ) while the average facet length  $f$  was also calculated. The average facet length  $f$  (corresponding to the mean distance between kinks) was also calculated using the expression  $f = L/N_{pk}$  (where  $L$  is the system size and  $N_{pk}$  is the number of local maxima) as a function of thickness for both discrete models in order to obtain the facet coarsening exponent  $\delta$ , where  $f \sim \langle h \rangle^\delta$ . In order to obtain good statistics, simulations were carried out with large system sizes ( $L=65536$ ).

Fig. 5 shows our results for the surface width as a function of film thickness  $\langle h \rangle$  for both discrete models. Although the surface is significantly rougher than in the

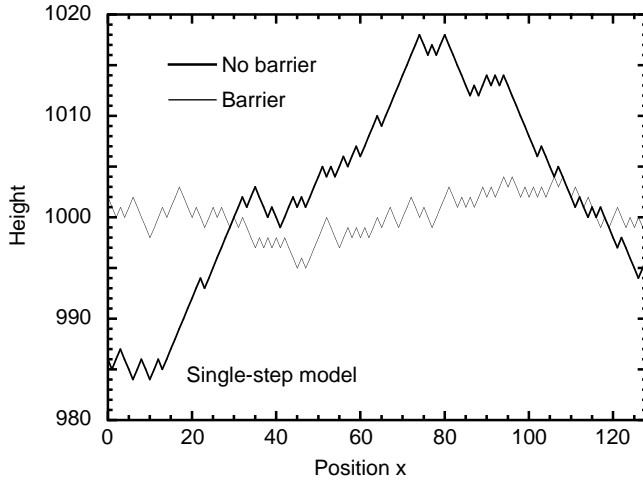


Fig. 6. Surface morphology obtained from single-step model after 1000 layers have been deposited (system size  $L = 256$ ).

continuum model due to the presence of kinks along the sides of the mounds (see Fig. 6), in the absence of a barrier to interfacet diffusion we obtain  $\beta = \frac{1}{3}$ , in agreement with our continuum model results and the scaling argument prediction [20]. Similar results for the lateral coarsening behavior (not shown), i.e., a well-defined lateral feature size  $r_c$  and a coarsening exponent  $n \simeq \frac{1}{3}$ , were also obtained. Thus, in the absence of an interfacet diffusion barrier, well-defined mounds are formed, while the coarsening behavior is in agreement with the scaling arguments of Ref. [20]. In contrast, as shown in Fig. 5, in the presence of a barrier to interfacet diffusion we find  $\beta \simeq \frac{1}{4}$ . In this case, there is no well-defined lateral feature size and the surface is self-affine as shown in Fig. 6. Such behavior may be explained by the presence of a downhill current [29] due to the combination of the interfacet diffusion barrier and the single-step restriction. Such a downhill current leads to a positive surface tension and Edwards–Wilkinson scaling behavior [25].

Fig. 7 shows our results for the facet length  $f$  as a function of film thickness. As can be seen, in the presence of a barrier to interfacet diffusion, the average facet length is essentially constant. The value in this case ( $f \simeq 3$ ) is close to that expected for a random walk of up and down steps, which is consistent with Edwards–Wilkinson scaling behavior in two dimensions. In contrast, in the absence of a barrier to interfacet diffusion, the average facet length  $f$  increases logarithmically with film thickness. The slow growth of the facet length in this case justifies our assumption of negligible island nucleation and may also help to explain why, even if the nucleation length is relatively short compared to the mound size, relatively well-defined facets are typically observed in polycrystalline growth. We note that if single kinks (corresponding to an up step in a sequence of down steps or a down step in a sequence of up steps) are neglected, then the average facet length becomes much larger (see Fig. 6) and increases as  $f \sim \langle h \rangle^{1/3}$  which is consistent with the observed mound coarsening behavior.

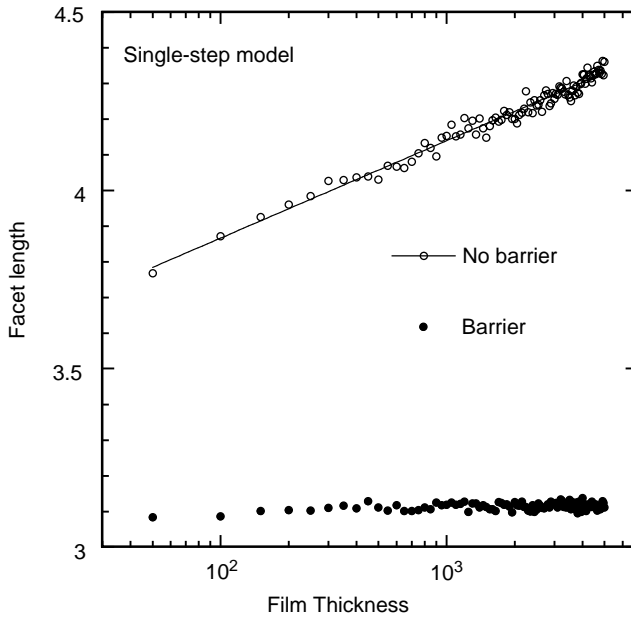


Fig. 7. Semilogarithmic plot of average facet length  $f$  as a function of film thickness.

#### 4. Discussion

We have developed and implemented both discrete and continuum models in order to study the effects of deposition noise on two-dimensional mound coarsening. Using our continuum ghost-particle model, we have demonstrated, in agreement with the scaling arguments put forward by Tang [20], that in the presence of deposition noise and angle selection but in the absence of thermal detachment and island nucleation, the coarsening exponent for two-dimensional mound coarsening is  $n = \frac{1}{3}$ . Our ‘ghost-particle’ model may also be viewed as a model of polycrystalline growth for the case in which there is only one preferred facet angle.

In order to better understand the relationship between microscopic growth mechanisms and the overall coarsening behavior, we have also studied two discrete models corresponding to a ‘conserved’ single-step model with surface diffusion. These models may also be thought of as two-dimensional models of faceted growth. Our results indicate that relatively subtle changes in the diffusion dynamics can lead to very large differences in the morphology and coarsening behavior. In particular, we found that in the presence of a strong barrier to interfacet diffusion, the surface is self-affine and Edwards–Wilkinson behavior ( $\beta = \frac{1}{4}$ ) is obtained. In contrast, in the absence of such a barrier, well-defined mounds are observed and the mound coarsening behavior is the same as in the continuum model. Since even a relatively weak barrier to interfacet diffusion will lead to a net downhill current, we expect that in general, well-defined mounds will only occur asymptotically in the absence of such a barrier. However, the



crossover thickness before the self-affine behavior becomes manifest may be relatively large. Exploring the dependence of such a crossover on the strength of the interfacet barrier is a challenge for future work.

Interestingly, we also found that in the absence of an interfacet diffusion barrier, the mean facet length, corresponding to the mean distance between kinks, increases logarithmically with film thickness. This behavior is most likely related to the known logarithmic coarsening which occurs for one-dimensional phase separation [30] and two-dimensional mound coarsening [23] in the absence of noise. In particular, while deposition noise leads to an initially random distribution of kinks, in the limit of large film thickness and facet length, the deposition noise becomes increasingly irrelevant as far as the microscopic kink motion is concerned. However, the remaining fluctuations play an important role in mound coalescence and lead to mound coarsening with  $n = \frac{1}{3}$ .

It is also interesting to compare our continuum model with the discrete model in the presence of a strong interfacet diffusion barrier. As can be seen by comparing the growth mechanisms for both models (Figs. 1 and 4), the differences are relatively small, despite the large difference in the coarsening behavior. In particular, while both models allow mass redistribution along facets, for sufficiently large facets growth only occurs on the facet on which deposition takes place or on a neighboring facet ‘in the same valley’. However, in the continuum model arbitrarily small facets may occur as shown in Fig. 2(b). Deposition on such facets may lead to ‘overrunning’ of the neighboring facets as shown in Fig. 1(b), just as in the discrete model without a barrier. The existence of such events may thus explain the large coarsening exponent observed in the continuum model.

Finally, we note that our results may lead to the development of improved continuum and discrete models of polycrystalline growth. For example, the van der Drift model [31], has been used to study the deterministic evolution of polycrystalline thin films with random crystalline orientation in two and three dimensions [32–35]. In the future, it may be possible to extend these results to include the effects of deposition noise and/or shadowing on the coarsening behavior.

## Acknowledgements

J.G. Amar would like to acknowledge support from the Petroleum Research Fund of the American Chemical Society as well as a grant of computer time from the Ohio Supercomputer Center. D.J. Baxter was supported by an NSF grant from the University of Toledo Summer 2000 REU program.

## References

- [1] J.Y. Tsao, *Material Fundamentals of Molecular Beam Epitaxy*, World Scientific, Singapore, 1993.
- [2] A.-L. Barabasi, H.E. Stanley, *Fractal Concepts in Surface Growth*, Cambridge University Press, New York, 1995.
- [3] M.D. Johnson, C. Orme, A.W. Hunt, D. Graff, J. Sudijono, L.M. Sander, B.G. Orr, *Phys. Rev. Lett.* 72 (1994) 116.

- [4] J.E. Van Nostrand, S. Jay Chey, M.-A. Hasan, D.G. Cahill, J.E. Greene, *Phys. Rev. Lett.* 74 (1995) 1127.
- [5] J.E. Van Nostrand, S. Jay Chey, D.G. Cahill, *Phys. Rev. B* 57 (1998) 12536.
- [6] J.A. Stroschio, D.T. Pierce, M. Stiles, A. Zangwill, L.M. Sander, *Phys. Rev. Lett.* 75 (1995) 4246; K. Thürmer, R. Koch, M. Weber, K.H. Rieder, *Phys. Rev. Lett.* 75 (1995) 1767.
- [7] F. Tsui, J. Wellman, C. Uher, R. Clarke, *Phys. Rev. Lett.* 76 (1996) 3164.
- [8] H.-J. Ernst, F. Fabre, R. Folkerts, J. Lapujoulade, *Phys. Rev. Lett.* 72 (1994) 112; W.C. Elliott, P.F. Miceli, T. Tse, P.W. Stephens, *Phys. Rev. B* 54 (1996) 17938; B.W. Karr, D.G. Cahill, J.E. Greene, *Appl. Phys. Lett.* 70 (1997) 1703.
- [9] L.C. Jorritsma, M. Bijmagne, G. Rosenfeld, B. Poelsema, *Phys. Rev. Lett.* 78 (1997) 911.
- [10] J.-K. Zuo, J.F. Wendelken, *Phys. Rev. Lett.* 78 (1997) 2791.
- [11] J. Alvarez, E. Lundgren, X. Torrelles, S. Ferrer, *Phys. Rev. B* 57 (1998) 6325.
- [12] C.E. Botez, P.F. Miceli, P.W. Stephens, *Phys. Rev. B* 64 (2001) 125427.
- [13] C.R. Stoldt, K.J. Caspersen, M.C. Bartelt, C.J. Jenks, J.W. Evans, P.A. Thiel, *Phys. Rev. Lett.* 85 (2000) 800; K.J. Caspersen, C.R. Stoldt, A.R. Layson, M.C. Bartelt, P.A. Thiel, J.W. Evans, *Phys. Rev. B* 63 (2001) 085401.
- [14] J. Villain, *J. Phys. I (France)* 1 (1991) 19; J. Krug, M. Plischke, M. Siegert, *Phys. Rev. Lett.* 70 (1993) 3271.
- [15] G. Ehrlich, F. Hudda, *J. Chem. Phys.* 44 (1966) 1039; R.L. Schwoebel, *J. Appl. Phys.* 40 (1969) 614.
- [16] J.G. Amar, F. Family, *Phys. Rev.* 54 (1996) 14742.
- [17] J.G. Amar, *Phys. Rev. B* 60 (1999) R11317.
- [18] M. Siegert, *Phys. Rev. Lett.* 81 (1998) 5481.
- [19] D. Moldovan, L. Golubovic, *Phys. Rev. E* 61 (2000) 6190.
- [20] L.-H. Tang, *Physica A* 254 (1998) 135.
- [21] L.-H. Tang, P. Smilauer, D.D. Vvedensky, *Eur. Phys. J. B* 2 (1998) 409.
- [22] M. Siegert, M. Plischke, *Phys. Rev. Lett.* 73 (1994) 1517.
- [23] P. Politi, J. Villain, *Phys. Rev. B* 54 (1996) 5112.
- [24] W.W. Mullins, *J. Appl. Phys.* 28 (1957) 333.
- [25] S.F. Edwards, D.R. Wilkinson, *Proc. Roy. Soc. London A* 381 (1982) 17.
- [26] P. Meakin, P. Ramanlal, L.M. Sander, R.C. Ball, *Phys. Rev. A* 34 (1986) 5091.
- [27] J.G. Amar, F. Family, *Phys. Rev. B* 54 (1996) 14071.
- [28] J.G. Amar, F. Family, *Phys. Rev. Lett.* 77 (1996) 4584.
- [29] F. Family, *J. Phys. A* 19 (1986) L441.
- [30] K. Kawasaki, T. Ohta, *Physica A* 116 (1982) 573.
- [31] A. van der Drift, *Philips Res. Rep.* 22 (1967) 267.
- [32] A.N. Kolmogorov, *Dokl. Akad. Nauk SSSR* 65 (1949) 681.
- [33] J.M. Thijssen, H.J.F. Knops, A.J. Dammers, *Phys. Rev. B* 45 (1992) 8650.
- [34] J.M. Thijssen, *Phys. Rev. B* 51 (1995) 1985.
- [35] Paritosh, D.J. Srolovitz, C.C. Battaile, et al., *Acta Mater.* 47 (1999) 2269.